

AFRL-AFOSR-UK-TR-2010-0003



Development of Novel Skin Materials for Morphing Aircraft

**Venkata P Potluri
University of Manchester
School of Materials
Sackville Street Building
Manchester, Greater Manchester
United Kingdom M60 1QD**

EOARD GRANT 083083

19 November 2010

Final Report for 15 September 2008 to 15 November 2010

Distribution Statement A: Approved for public release distribution is unlimited.

**Air Force Research Laboratory
Air Force Office of Scientific Research
European Office of Aerospace Research and Development
Unit 4515 Box 14, APO AE 09421**

REPORT DOCUMENTATION PAGE				Form Approved OMB No. 0704-0188	
Public reporting burden for this collection of information is estimated to average 1 hour per response, including the time for reviewing instructions, searching existing data sources, gathering and maintaining the data needed, and completing and reviewing the collection of information. Send comments regarding this burden estimate or any other aspect of this collection of information, including suggestions for reducing the burden, to Department of Defense, Washington Headquarters Services, Directorate for Information Operations and Reports (0704-0188), 1215 Jefferson Davis Highway, Suite 1204, Arlington, VA 22202-4302. Respondents should be aware that notwithstanding any other provision of law, no person shall be subject to any penalty for failing to comply with a collection of information if it does not display a currently valid OMB control number.					
1. REPORT DATE (DD-MM-YYYY) 19-11-2010		2. REPORT TYPE Final Report		3. DATES COVERED (From – To) 15 September 2008 – 15 November 2010	
4. TITLE AND SUBTITLE Development of novel skin materials for morphing aircraft			5a. CONTRACT NUMBER FA8655-08-1-3083		
			5b. GRANT NUMBER		
			5c. PROGRAM ELEMENT NUMBER		
6. AUTHOR(S) Dr. Venkata P Potluri			5d. PROJECT NUMBER		
			5d. TASK NUMBER		
			5e. WORK UNIT NUMBER		
7. PERFORMING ORGANIZATION NAME(S) AND ADDRESS(ES) University of Manchester Sackville street building Manchester M60 1QD United Kingdom				8. PERFORMING ORGANIZATION REPORT NUMBER Grant 08-3083	
9. SPONSORING/MONITORING AGENCY NAME(S) AND ADDRESS(ES) EOARD Unit 4515 BOX 14 APO AE 09421				10. SPONSOR/MONITOR'S ACRONYM(S)	
				11. SPONSOR/MONITOR'S REPORT NUMBER(S) AFRL-AFOSR-UK-TR-2010-0003	
12. DISTRIBUTION/AVAILABILITY STATEMENT Approved for public release; distribution is unlimited.					
13. SUPPLEMENTARY NOTES					
14. ABSTRACT This project explored development of 'skin' material for morphing structures. Flexible fiber-reinforced composites are the prime candidates for morphing skins in order to achieve the required elongation and strength. Main objective was to develop a woven or cross ply fabric that can exhibit extension as well as shear deformations by developing and incorporating hyper-elastic yarns. These yarns consist of low modulus elastomeric core braided with high-modulus fibers. Low-modulus phase allows significant area change during deployment, and the high modulus stage provides the necessary stiffness to the skin after deployment. The 'knee-point' can be tuned to the desired strain necessary for the application by altering the manufacturing settings. In this work, two different hyper-elastic yarns were produced: biaxial braids and triaxial braids. Tensile testing showed the deformation processes to be similar. However, due to the style of interlacement, triaxial yarns achieved larger extensions. Both the styles of yarn are suitable for morphing skin applications. In addition, various braided yarns were developed by changing the pre-tension on the elastane yarn to produce different braid angles. The knee-point between low modulus and high modulus behavior was shown to shift based on braid angle, allowing a means of tuning the desired strain. A computational model for predicting the load-strain behavior of hyper-elastic yarns was developed and shown to agree well with experimental results. Finally, a woven composite was manufactured and tested as a morphing skin material using the braided yarns, and compared to analytical mechanics-based predictions.					
15. SUBJECT TERMS EOARD, morphing structures, morphing skins					
16. SECURITY CLASSIFICATION OF:			17. LIMITATION OF ABSTRACT UL	18. NUMBER OF PAGES 22	19a. NAME OF RESPONSIBLE PERSON Randall Pollak, Lt Colonel, USAF
a. REPORT UNCLAS	b. ABSTRACT UNCLAS	c. THIS PAGE UNCLAS			19b. TELEPHONE NUMBER <i>(Include area code)</i> +44 (0)1895 616 115



DEVELOPMENT OF MORPHING SKINS

Principal Investigator: Dr Prasad Potluri

Graduate student: Miss Sabahat Nawaz

Research Associates: Dr Haseeb Arshad, Dr Raj Ramgulam

AFRL co-ordinator: Dr Jeff Baur

Grant: FA8655-08-3083

DEVELOPMENT OF MORPHING SKINS

Morphing Aircraft

A morphing aircraft can be defined as an aircraft that changes configuration to maximize its performance at radically different flight conditions. These configuration changes can take place in any part of the aircraft, e.g. fuselage, wing, engine, and tail. Wing morphing is naturally the most important aspect of aircraft morphing as it dictates the aircraft performance in a given flight condition, and has been of interest to the aircraft designers since the beginning of the flight, progressing from the design of control surfaces to the variable-sweep wing. Recent research efforts (mainly under DARPA and NASA sponsorships) however, are focusing on even more dramatic configuration changes such as 200% change in aspect ratio, 50% change in wing area, 5° change in wing twist, and 20° change in wing sweep to lay the ground work for truly multi-mission aircraft. Such wing geometry and configuration changes, while extremely challenging, can be conceptually achieved in a variety of ways – folding, hiding, telescoping, expanding, and contracting a wing, coupling and decoupling multiple wing segments.

Morphing structures require a large aspect ratio and area change during flight in order to optimise operational performance. Following are the key elements of a morphing wing concept:

- ***Skeleton***: a spatial kinematic linkage for achieving desired wing configurations by folding, telescoping, expanding or contracting
- ***Actuators*** for configuration change
- ***Skin***: To provide an aerodynamic surface free from wrinkles by accommodate large surface area changes.
- Means of ***rigidizing*** the skin

This project focuses on the development of ‘**skin**’ material. Key Requirements for the skin material are:

- ♦ Large area change
- ♦ Smooth aerodynamic surface, free from wrinkles
- ♦ Low creep under tension
- ♦ Low hysteresis in extension

- ♦ Convenient method of joining to the skeleton
- ♦ Suitable means of integration of digitization elements

Shear vs extensional modes

Flexible fibre reinforced composites are the prime candidates for morphing skins in order to achieve the required elongation and strength. There are two principal methods of achieving area change in an elastic membrane, shear mode and extensional mode. A biaxial fibre architecture, woven or cross-ply, exhibits reduction in surface area when deformed in shear - deformation along the yarn directions is insignificant (figure 1a). A knitted architecture (figure 1b) exhibits increase in surface area when stretched in principal and bias directions. However, knitted fabrics have limitations: limited range of elongations, significant knockdown in strength due to sharp curvatures, and difficulty in knitting high modulus yarns.

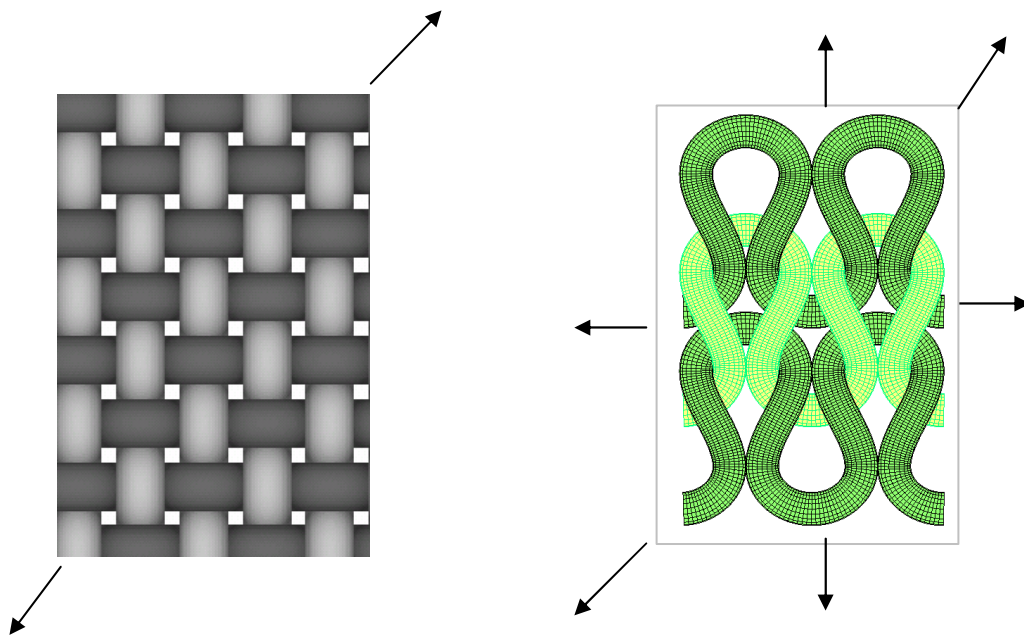


Figure 1: a) Shear mode b) extension mode

Concept of biaxial fabrics for extension mode

Main objective of this research is to develop a woven or cross ply fabric that can exhibit extension as well as shear deformations. This concept requires the development of hyper-elastic yarns.

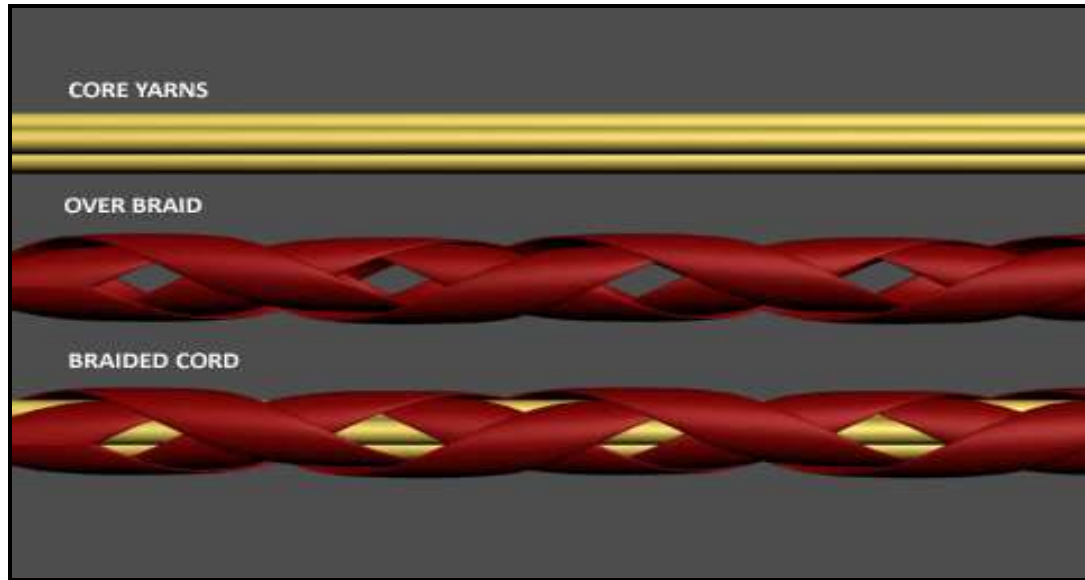


Figure 2: concept of hyper-elastic yarns

The concept of hyper-elastic yarns is shown in figure2. These yarns consist of low-modulus elastomeric core braided around with high-modulus fibres. Expected force-strain behaviour is as shown in figure 3. Low-modulus phase allows significant area change during deployment, and the high modulus stage provides the necessary stiffness to the skin after deployment. The ‘knee-point’ can be tuned to the required strain (by altering the manufacturing process).

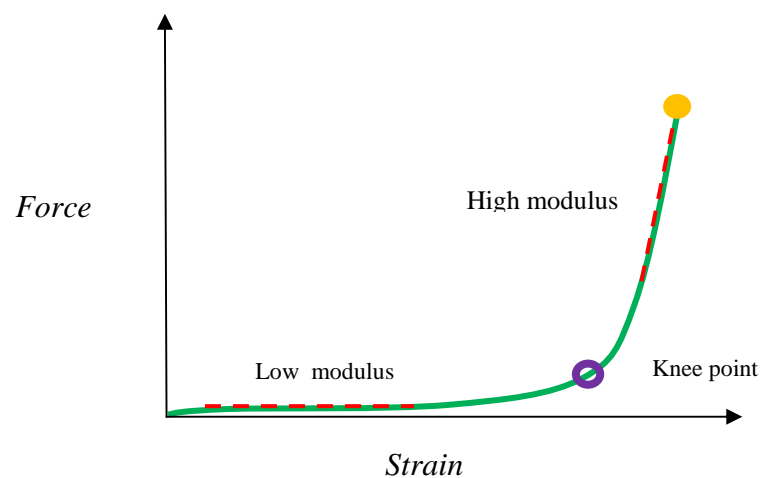


Figure 3: Force-strain behaviour of hyper-elastic yarns

Manufacture of hyper-elastic yarns

Hyper-elastic yarns have been produced on a braiding machine as per the figure 4. The elastomeric yarn passes through a tensioning device to stretch the yarn before passing through the braiding machine. Tension is also applied to the braid yarns to keep their let-off as smooth as possible. The yarns are pulled through the braiding machine by the take-up device. The elastomeric yarn and the braid yarn meet at the braid formation point (the point where the cord is formed), the cord is kept under tension until it passes through the take-up device; here the cord relaxes to give the final yarn structure.

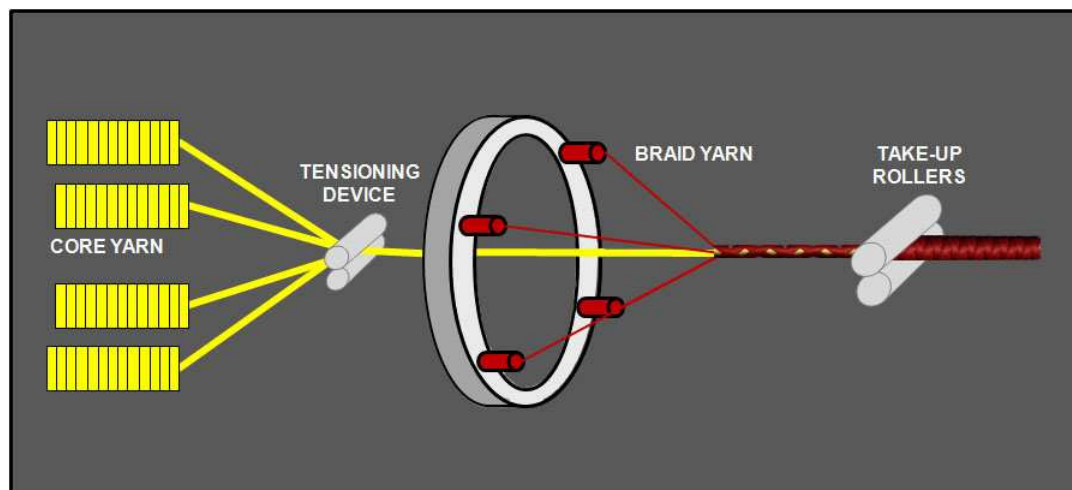


Figure 4: Typical set-up for a biaxial braid with core yarn

The braiding machine (with 24 yarn carriers) has been set-up with four carriers, this would be ideal to produce a thin light-weight cord, so only 4 braid yarns have been used. When braiding with an elastomeric core, in order to optimise the extension percentage with the most efficient production timing and product quality, you have to get the right balance between the elastomeric yarn delivery tension, the machine/yarn carrier speed, and the take up speed.

Pre-tensioning the elastomeric yarn influences the braid angle of the cord in the relaxed state because after the cord passes through the take-up rollers, the elastomeric yarn relaxes and the braid structure contracts. Therefore the cord in the relaxed state has a higher braid angle to the cord in the tensioned state.

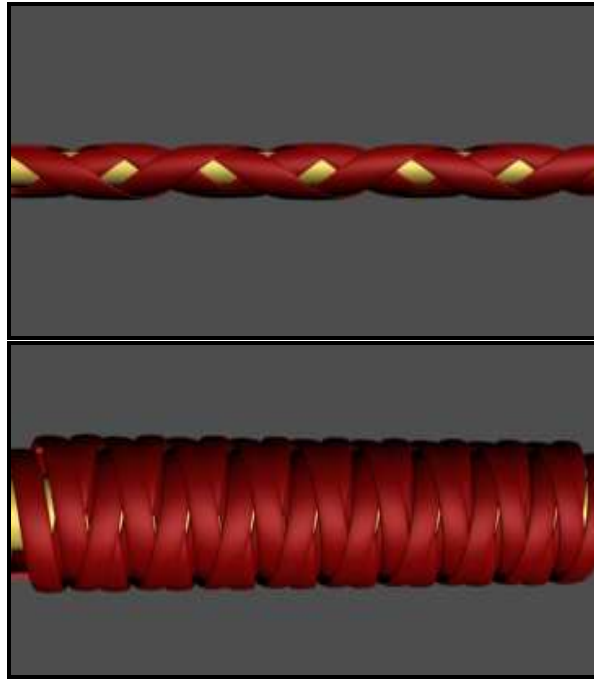


Figure 5: Cord during braiding in tensioned state vs. Cord in the relaxed state

The braid angle

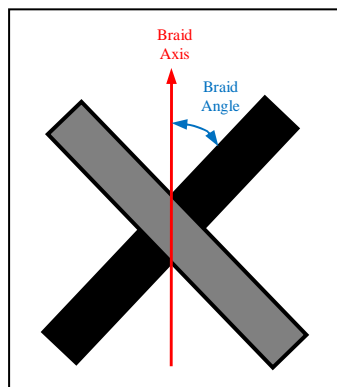


Figure 6: braid angle

The braid angle is the orientation of the yarns from the braid axis (figure6). Braid angle can be measured using image analysis. When extending a braided structure there is a kinematic rotation of reinforcing yarn as shown in figure 7. As the braided structure is pulled, the braid angle (θ) decreases, but the length of the wrap yarn (l_0) stays the same. However, the length of the braid increases from an initial length (l_1) to the extended position (l_2). But there is a limit to the amount which the braid can extend because the braid will eventually reach a ‘jamming position’ where the yarns will lock. Therefore maximum strain achieved by a braided yarn depends on the initial braid angle.

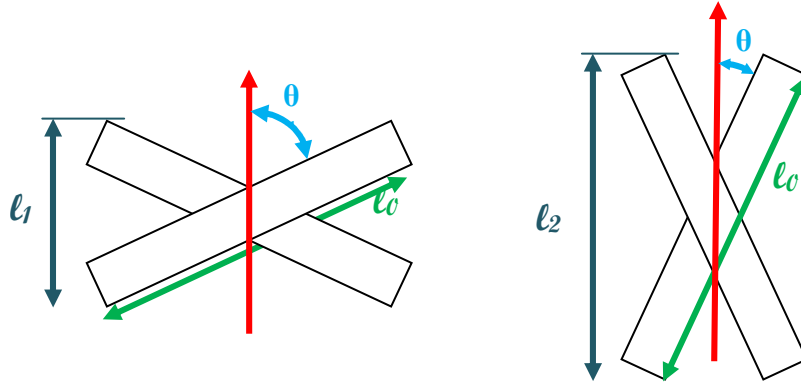


Figure 7: kinematic rotation of braided structure

In this work, two different hyper-elastic yarns were produced: 1) biaxial braids and 2) triaxial braids.

The biaxial elastomeric braid consists of 4 elastane yarns as the core and 4 Kevlar yarns for interlacing around the core yarns. Elastane yarns are passed through the centre of the braiding machine and the braid yarns intertwine around them, creating an overwrap of the braid yarns, placing the elastane in the centre. Figure 8 shows the braiding machine set-up for biaxial braids. It can be seen that the elastane core yarns pass through the centre of the machine, and the four Kevlar yarn bobbins are mounted on carriers that rotate on a track. Two of the carriers rotate in clock-wise direction interlacing with the two yarn carriers rotating in anti clock-wise direction.

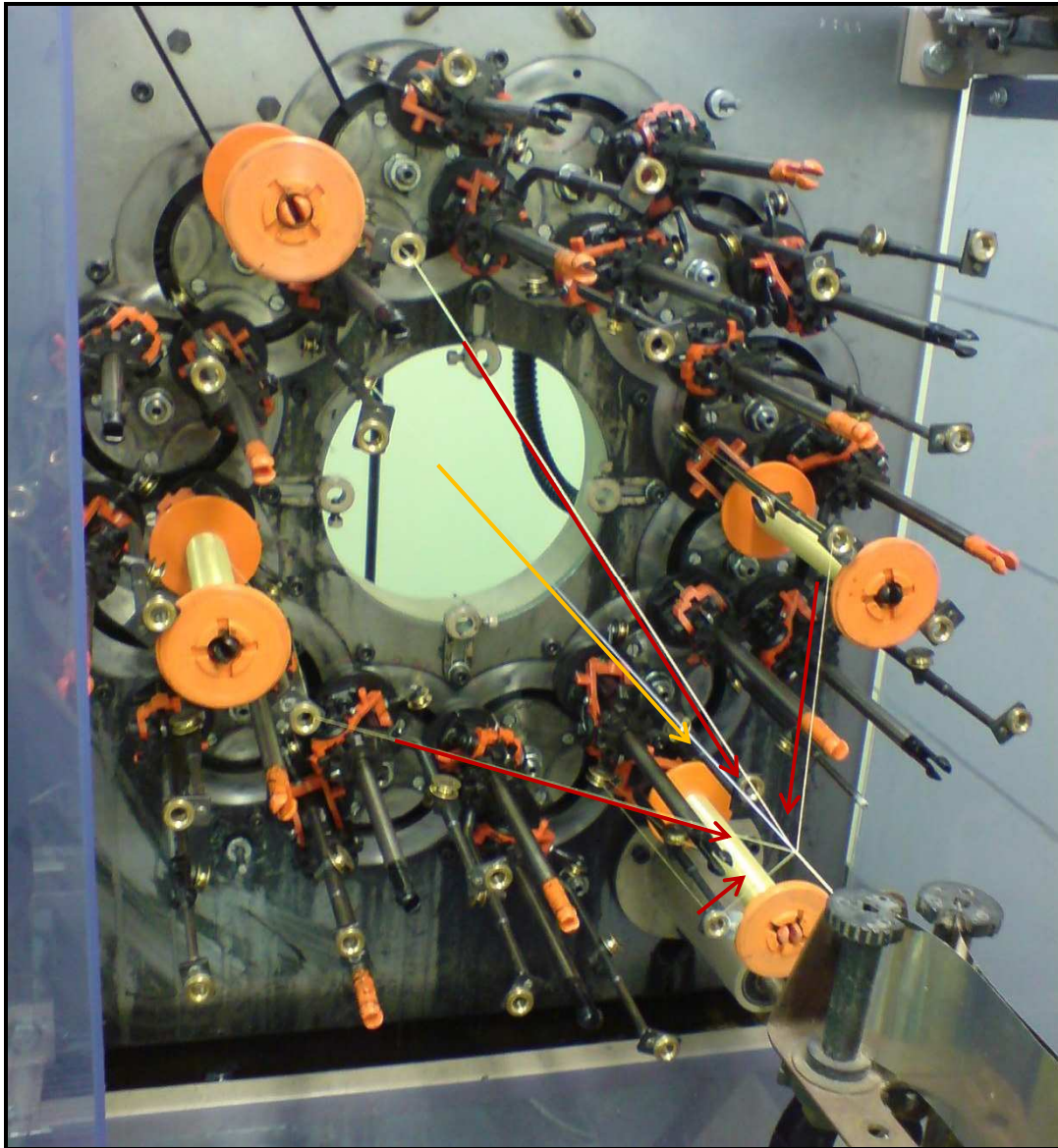


Figure 8: The braiding machine set up for the biaxial braid cord

Biaxial braided structure, as illustrated in figure 2, consist of straight core yarns wrapped around by interlacing braid yarns. Braid angle decreases with the elongation (figure 9) and reaches a locking limit.

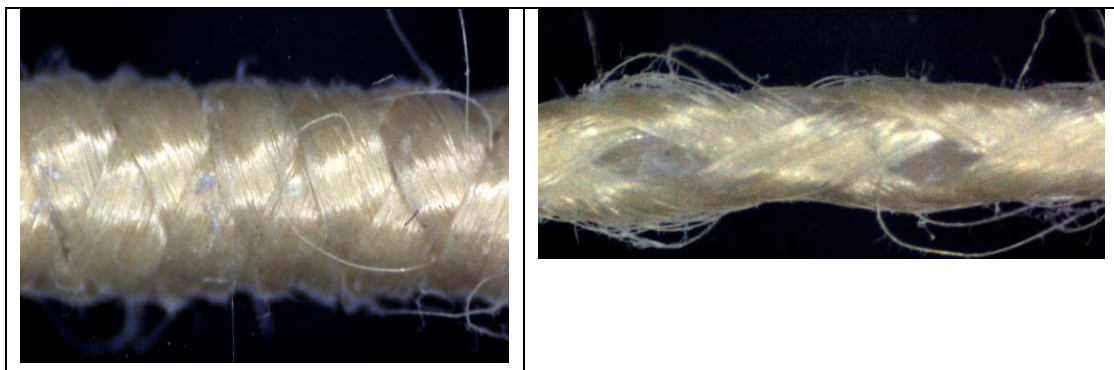


Figure 9: Biaxial braided structure before and after stretching

Triaxial braided structure consists of four straight elastane yarns and four Kevlar yarns interlacing around them. In a triaxial structure, straight yarns pass through the interlacing path of braided yarns (figure 10).

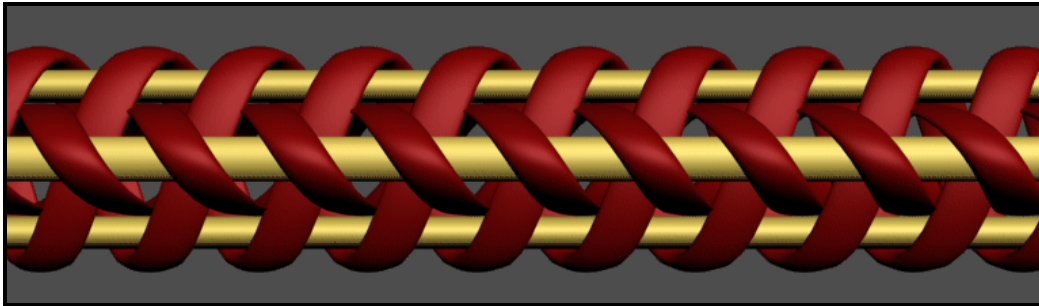


Figure 10: Triaxial braided structure

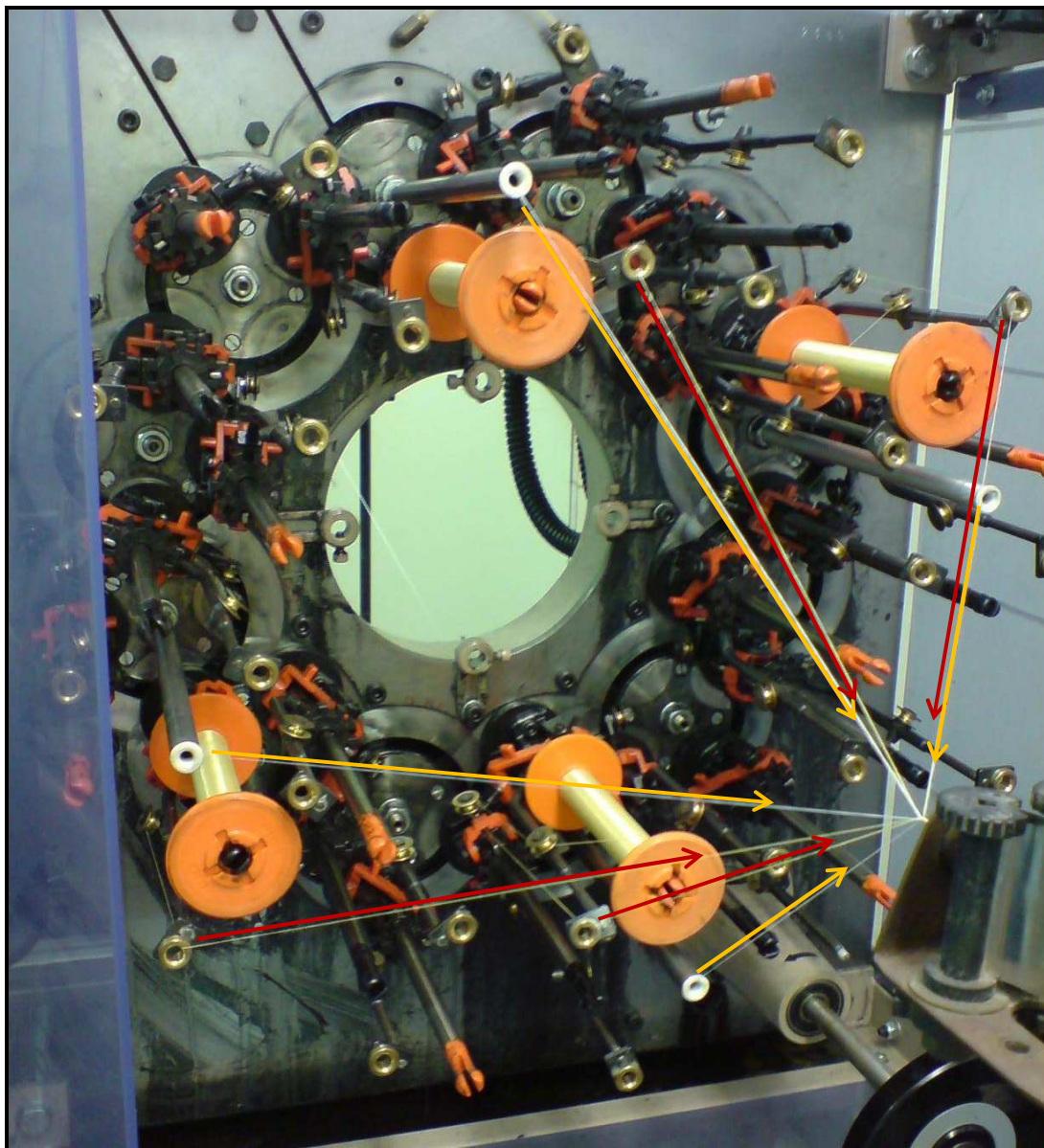


Figure 11: The braiding machine set up for the triaxial braid cord

The elastane yarns are passed through the centre of the horgears (which the braid yarn carriers rotate around) rather than through the machine centre; the braid yarns intertwine in between and around the elastane warp yarns and are incorporated inside the braid (figure 11).

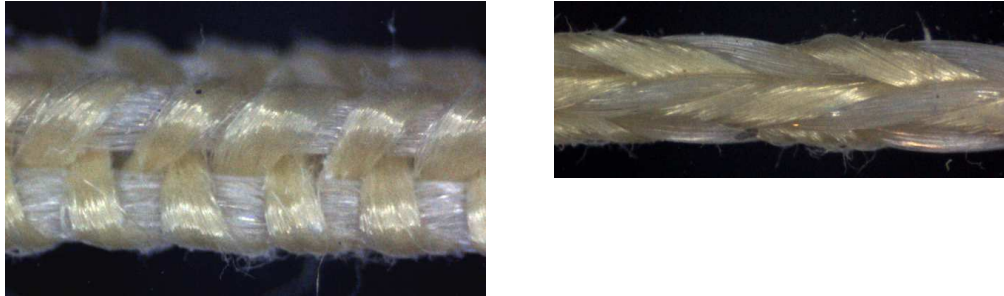


Figure12: triaxial braid in the relaxed before and after stretching

Load-elongation behaviour of hyper-elastic yarns

Deformation process of the triaxial yarns is very similar to biaxial yarns (figure13 &14). However, due to the style of interlacement, triaxial yarns can achieve larger extensions in comparison to biaxial yarns. Both the styles of yarn are suitable for the morphing skin applications. Figure 13 & 14 show the load-strain behaviour of biaxial and triaxial yarns.

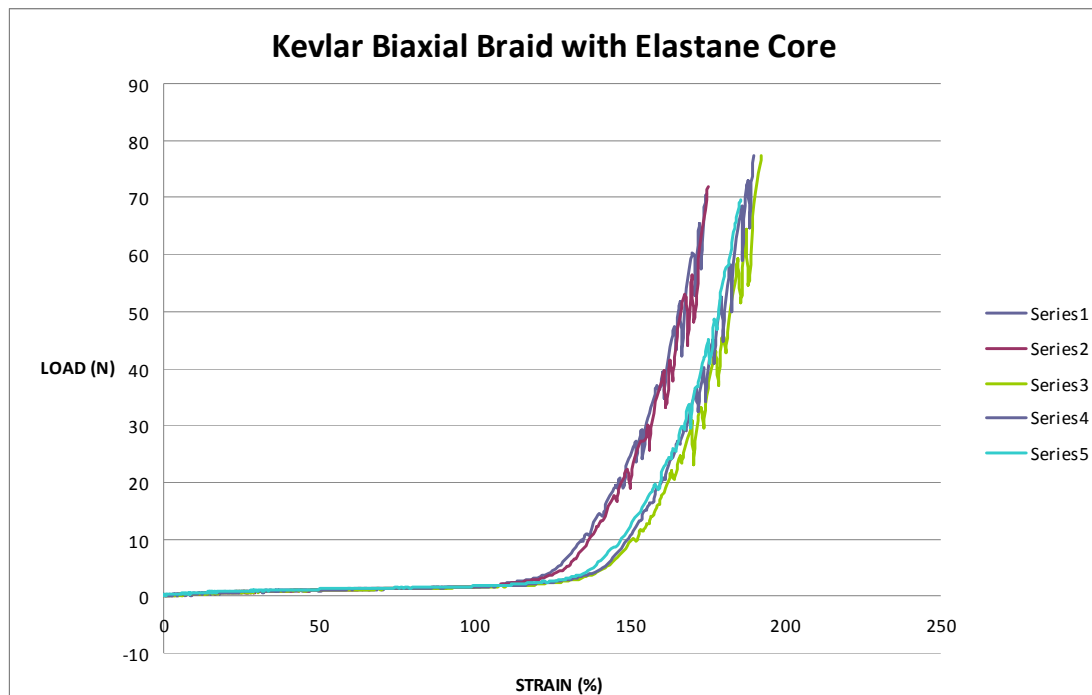


Figure 13: Load strain curves for biaxial braids

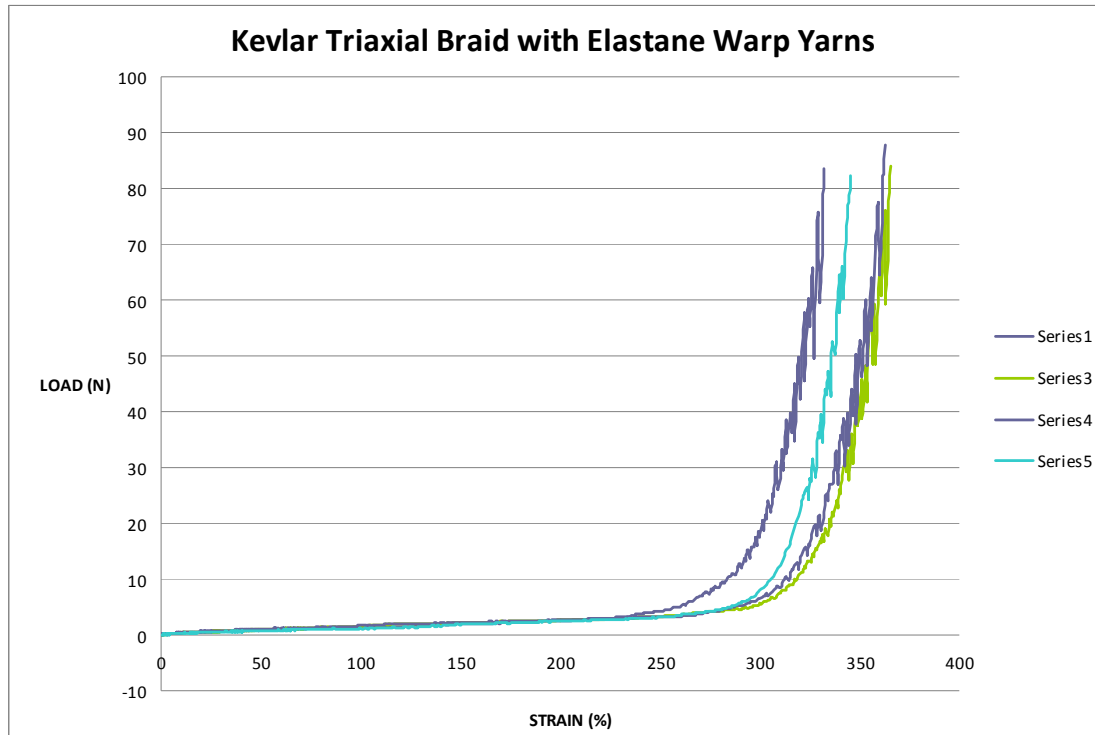


Figure 14: Load-strain curves for triaxial braids

Development of braided yarns with different strain limits

Four different braided yarns were developed (by changing the pre-tension on the elastane yarn) with different braid angles.

Braid	Initial braid angle	Braid angle at the knee	Max strain %
Braid 1	29	27	22
Braid 2	38	27	49
Braid 3	52	27	89
Braid 4	73	27	254

Table 1: Relation between initial braid angle and maximum strain

It can be seen from figure 15 that the knee point on the graph can be shifted by changing the braid angle. Hence, it is possible to design a yarn with required load-strain relationship for a given state of deployment (of the morphing structure).

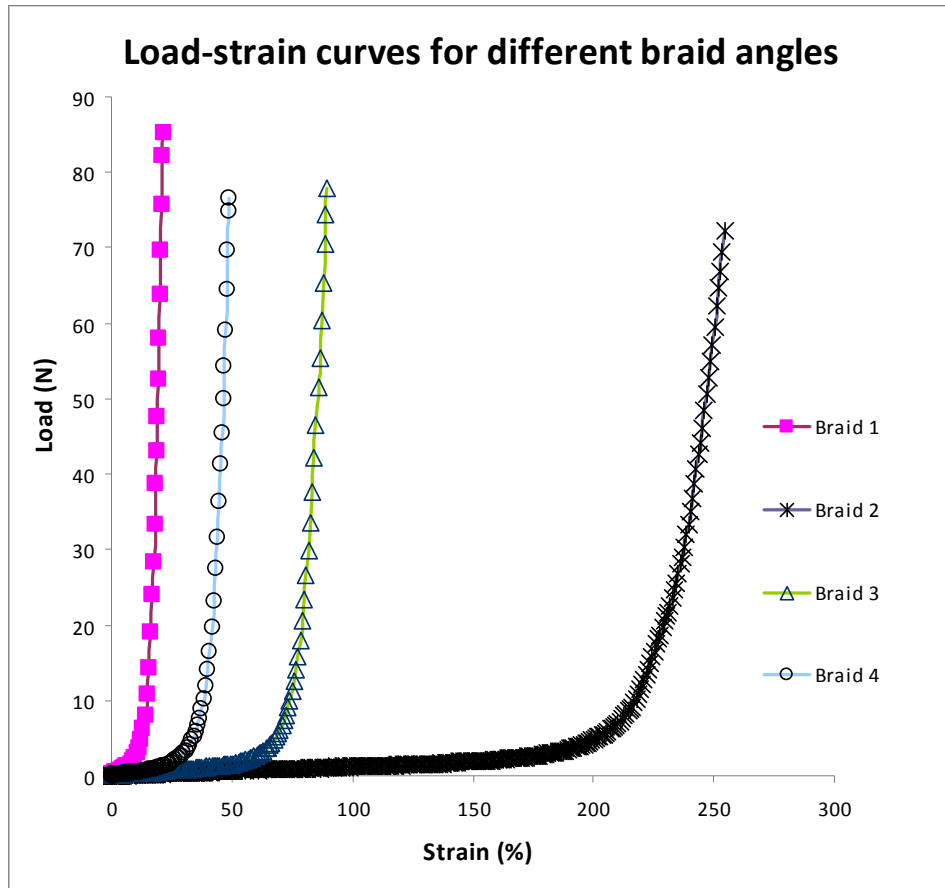


Figure 15: Load-strain relationship of braids with different braid angles

Modelling the load-elongation behaviour of hyper-elastic yarns

A computational model for predicting the load-strain behaviour of hyper-elastic yarns has been developed. The model is based on the principle of virtual work. The inputs to the model are:

- Stress-strain behaviour of elastane yarn
- Stress-strain behaviour of Kevlar yarn
- Yarn twist angle calculated from braid angle and core diameter
- Load-elongation characteristic of the filaments
- Poisson's ratio of the yarns

Load-strain behaviour of hyper-elastic braided yarns may be divided into three stages: Stage 1: low-modulus stage is dominated by elastane yarns. Kevlar yarns are subjected to kinematic rotation up to the knee point without significant contribution to the load/stress.

Yarn strain at the knee point can be computed using equation (1) based on kinematic rotations.

$$\varepsilon_{knee} = \frac{(\cos \theta_{knee} - \cos \theta_1)}{\cos \theta_1} \quad (1)$$

Force generated in the yarn is a function of elastane stress-strain curve.

Stage 2: from the knee point

Stage 2 of the load-deformation beyond knee point is dominated by complex interaction between the core and braided yarns. Mechanics of this stage was originally derived for spun yarns (figure 16) and subsequently modified for braided yarns.

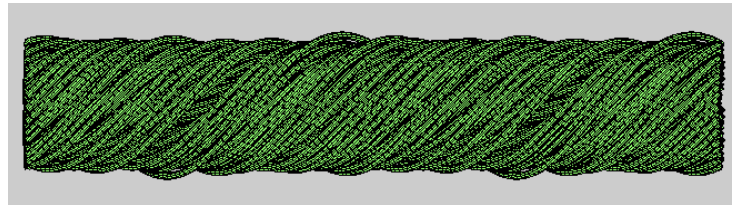


Figure 16: Geometry of Filaments in a yarn

Strain Analysis

The relationship between the strain in a filament, ε_i , when the yarn is subjected to a strain $\varepsilon_y = \frac{\partial u}{\partial s}$ is given as follows (s is length measured along yarn axis and u is the extension):

$$\varepsilon_i = \sqrt{(1 + \varepsilon_y^2) \cos^2 \alpha + (1 - \sigma \varepsilon_y^2) \sin^2 \alpha} - 1 \quad (2)$$

where

σ is the yarn Poisson ratio.

α is the helix angle

This relationship is valid for small strain values but more specifically it assumes that the helical angle of the filaments do not change with yarn deformation.

Energy Considerations: Virtual Work

Using the principle of virtual work the relationships between external forces and strains for the yarn are derived in the following analysis.

The incremental strain energy of a single filament is:

$$\delta U_i = \iiint_{v_i} \varepsilon_i \delta \varepsilon_i dv_i \quad (3)$$

where $dv = A \cdot \frac{s}{\cos \alpha}$

$$\delta U_i = EA \cdot \int_0^L \varepsilon_i \delta \varepsilon_i \frac{ds}{\cos \alpha} \quad (4)$$

(Note: L is an arbitrary length of yarn, generally one twist)

Substituting equation (1) in equation (4):

$$\delta U_i = A \cdot E \cdot \frac{\left(\sqrt{(1+\varepsilon_y)^2 \cos^2 \alpha + (1-\sigma \cdot \varepsilon_y)^2 \sin^2 \alpha} - 1 \right) \left(2(1+\varepsilon_y) \cos^2 \alpha - 2(1-\sigma \cdot \varepsilon_y) \sin^2 \alpha \cdot \sigma \right) L}{2 \cos \alpha \sqrt{(1+\varepsilon_y)^2 \cos^2 \alpha + (1-\sigma \cdot \varepsilon_y)^2 \sin^2 \alpha}} \frac{\delta(u)}{L} \quad (5)$$

Summing up for the filaments in the yarn:

$$\delta U = \sum_{i=1}^{K_n} \sum_{n=1}^N \delta U_i$$

N: number of layers in yarn

K: number of filaments in a given layer n.

Principle of stationary potential energy

$$\Pi = V + U$$

$$\delta \Pi = \delta V + \delta U$$

At equilibrium $\delta \Pi = 0$

The variation of potential energy of external torque is: $\delta V = -F \delta(\Delta \phi)$ (6)

Hence the axial tensile contribution of each filament is obtained by combining equations (4) & (5):

$$F = A \cdot E \cdot \frac{\left(\sqrt{(1+\varepsilon_y)^2 \cos^2 \alpha + (1-\sigma \cdot \varepsilon_y)^2 \sin^2 \alpha} - 1 \right) \left(2(1+\varepsilon_y) \cos^2 \alpha - 2(1-\sigma \cdot \varepsilon_y) \sin^2 \alpha \cdot \sigma \right)}{2 \cos \alpha \sqrt{(1+\varepsilon_y)^2 \cos^2 \alpha + (1-\sigma \cdot \varepsilon_y)^2 \sin^2 \alpha}} \quad (7)$$

The tensile contribution for each filament has to be added to obtain the tension/strain relationship for the whole yarn. Figure 17 presents the computed load-strain behaviour of four braided yarns (produced with different braid angles). These curves compare favourably with the experimental curves presented in figure 15.

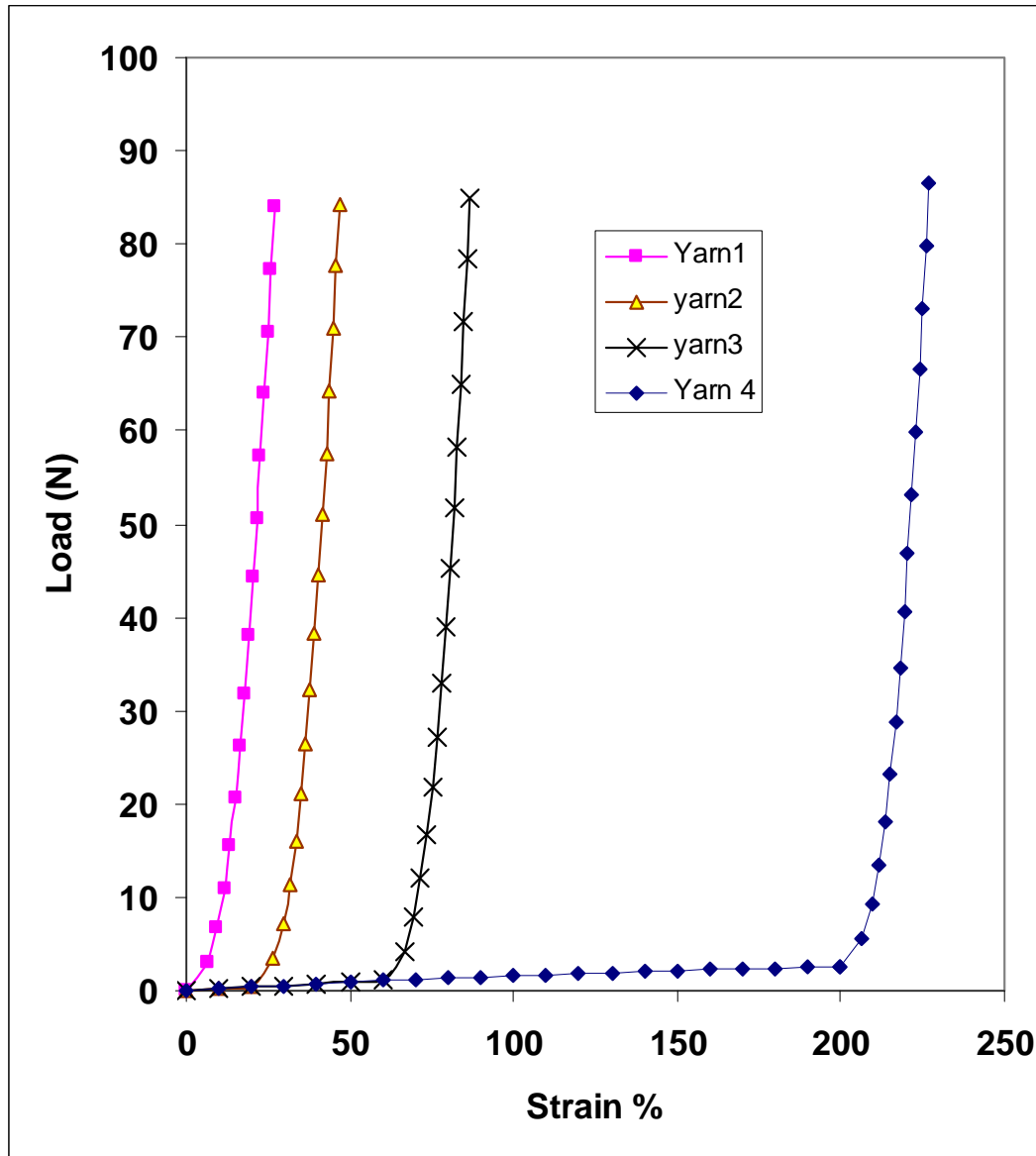


Figure 17: computed load-strain curves for hyper-elastic yarns

Computational model used in the present work for predicting the load-strain behaviour of the yarns is a useful tool in developing hyper-elastic yarns for specific extensibility.

Manufacture of morphing skin material

The fabric sample has a 1/1 plain weave, and is hand woven using a frame (figure 18) with removable bars to aid the removal of the samples from the frame. The vertical warp yarns are wrapped around the bars at intervals to give 2.5 ends/cm of fabric. The horizontal weft yarns are woven in and out of the warp yarns and around the wire rods to keep the structure of the fabric; the wefts are also inserted to give 2.5 picks/cm. This gives an even mesh-like fabric samples.

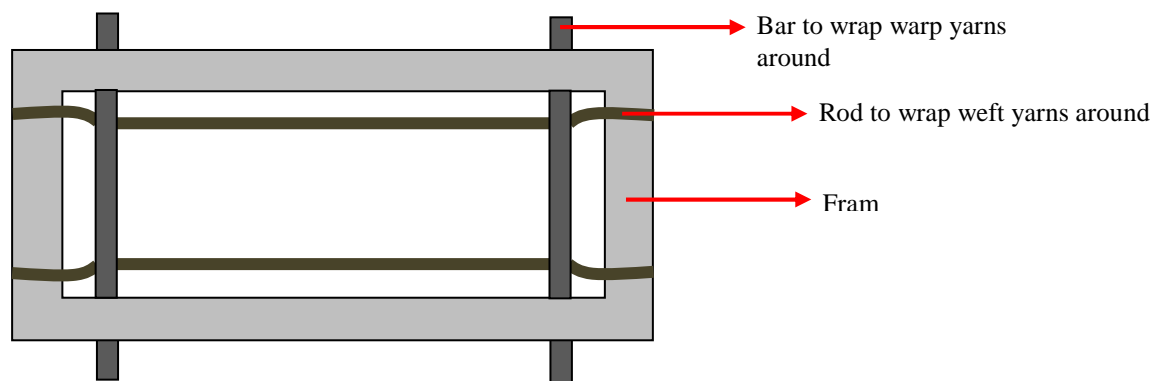


Figure 18: Weaving frame

A fabric sample woven with triaxial braided yarn is shown in figure 19.

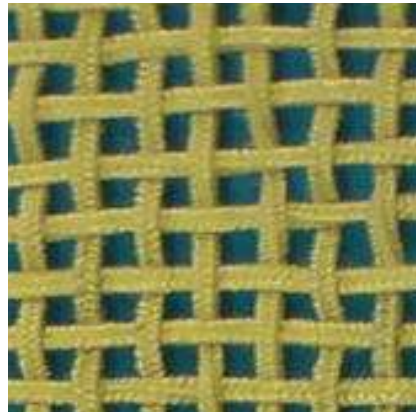


Figure 19: Woven fabric

As the samples are mesh structures, they need to be reinforced with a matrix material. We needed a matrix material that can cope with large deformations. We used soft silicone matrix for the present trials. Polyurethanes for example may be better suited for this application.

The silicone material comes in the form of a wet paste which allows it to be applied easily, and is self-curing. Initially a thin layer of silicone is spread on a non-stick sheet, then the fabric mesh sample (still inside the frame) is placed on top. Another layer of silicone is applied on top of the fabric, ensuring that the air gaps between the cords are filled. An additional non-stick sheet is placed on top of the sample. The assembly sample is placed in a press which has metal plates both on the bottom and on top. The sample is kept under constant pressure between these 2 plates until the silicone is fully cured. The sample is removed, and is easier to handle than the fabric without the matrix.



Figure 20: set-up for consolidation

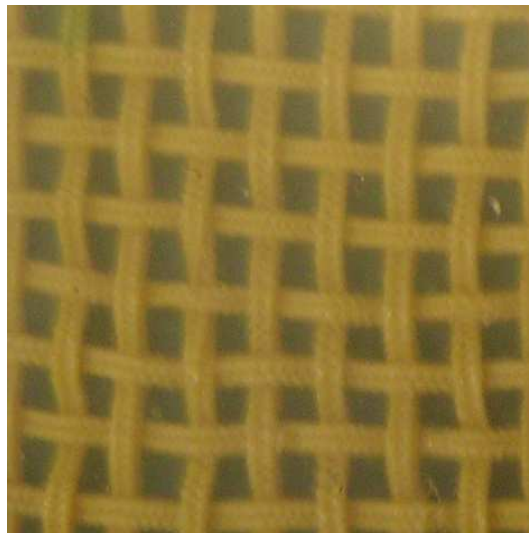


Figure 21: Flexible composite skin material

Stress-strain behaviour of skin material

Experimental stress-strain curve for the flexible composite (figure 21) is presented in figure 22. This material exhibits bilinear behaviour with low modulus up to a predetermined knee point (around 200%) and exhibits a high modulus beyond this point. Due to the slippery nature of the silicone material, it was not possible to test the sample until failure. In future trials, we will use a stiffer polymer (eg. PU) for the matrix in order to improve the initial modulus and the strength.

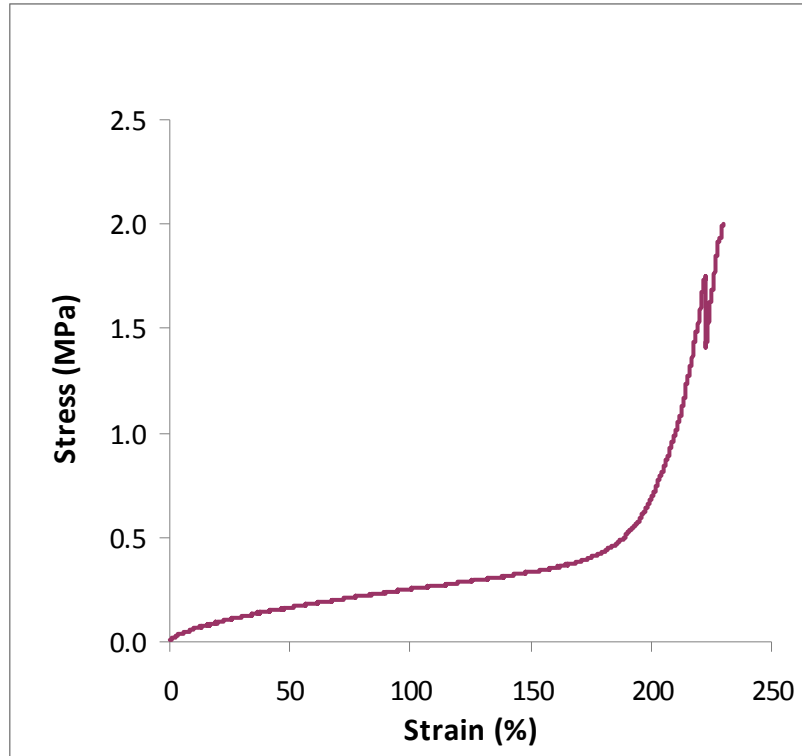


Figure 22: Experimental Stress-strain behaviour of the skin material

Mechanics of flexible composites

The fabric tensile model treats yarns in a plain weave structure as extensible elasticas which are basically long slender bodies bent in a principal plane by application of force. It involves solving a system of first order linear differential equations using advanced integration techniques.

The starting point of the analysis of ‘elastica’ is the Bernoulli-Euler law which states that bending moment at any point of the central line of a slender body is proportional to the curvature caused:

$$M = E_b \cdot k$$

Where M is the bending moment;

k is the curvature of the central line;

E_b is the bending rigidity.

The equilibrium of forces on an element of a yarn within a unit repeat can be considered. These forces result when a stretching (tensile) force P is applied. $2Q$ is the resultant of the reaction forces from crossing threads.

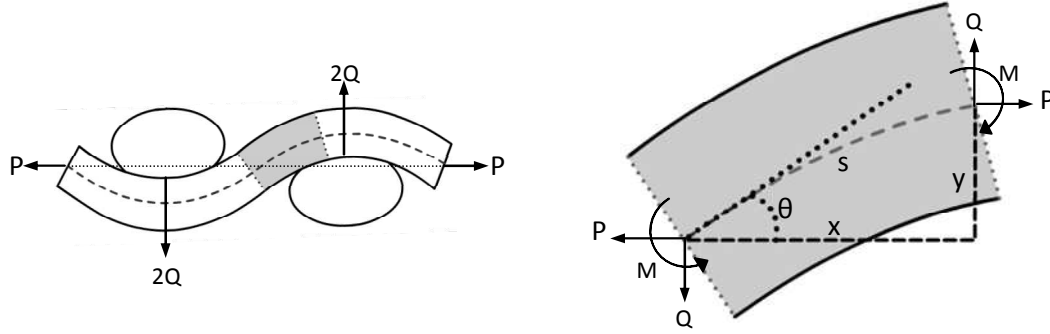


Figure 23 Equilibrium of forces on yarn element within unit repeat

Moment equilibrium gives the following differential equation:

$$E_b \frac{d^2\theta}{ds^2} + P \cdot \sin\theta - Q \cdot \cos\theta = 0$$

where, s is the length of the centre line of the deformed elastica, thus curvature is $\frac{d\theta}{ds}$

Measured yarn properties and dimensions, and geometric parameters relating to the fabric structure are used as inputs. These include: fabric sett, yarn crimp, number of filaments per yarn, and minimum & maximum yarn diameters. The rate of change of modulus with strain and the failure load are computed from experimental data relating yarn tensile stress and strain. Fabric tensile load-extension is simulated as an output.

The model also incorporate simple rule of mixture for incorporating matrix properties into mechanics of flexible woven fabric. Figure 24 compares the predicted stress-strain behaviour with the experimental curve. Experimental knee point is somewhat smaller than the computed – the difference is primarily due to reduced mobility of Kevlar yarn inside the matrix. Figure 25 shows the influence of matrix stiffness on the stress-strain behaviour. It is possible to tune the initial modulus, knee position, final modulus and strength of the flexible skin material.

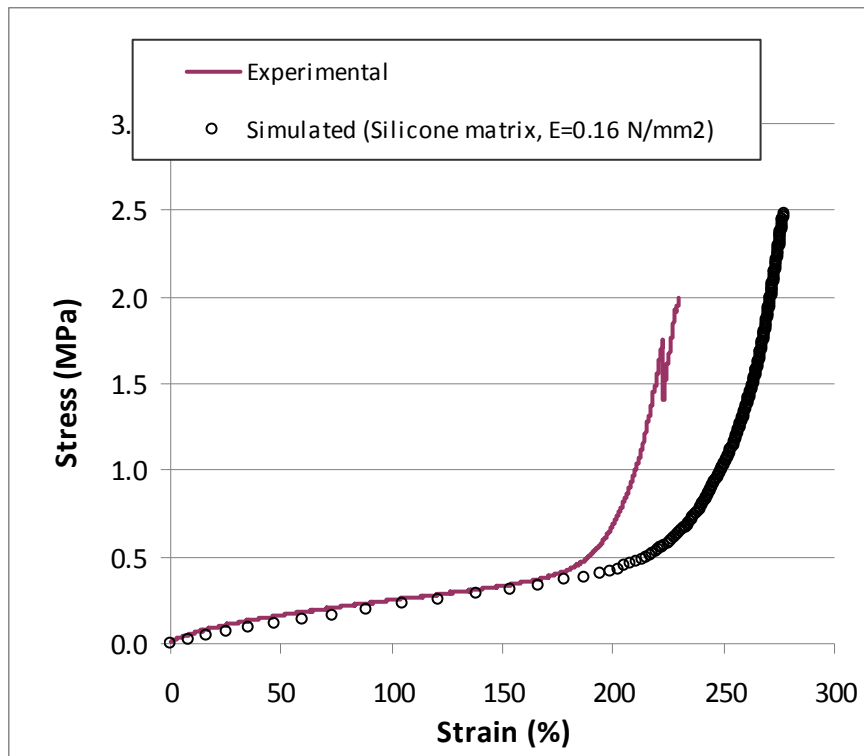


Figure 24: predicted versus experimental stress-strain curve

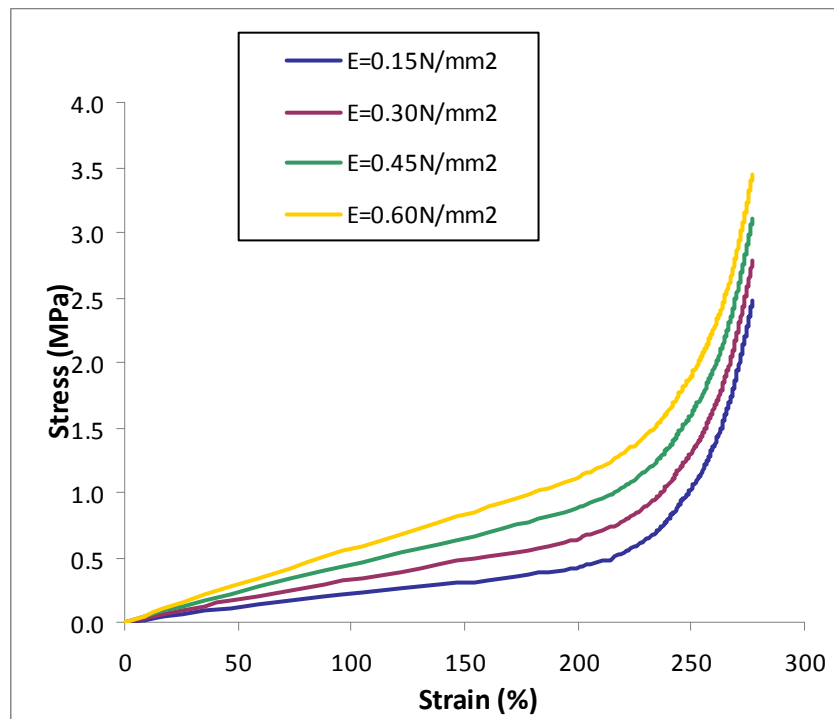


Figure 25: Influence of matrix stiffness on the stress-strain behaviour